

OCT Angiography–Based Detection and Quantification of the Neovascular Network in Exudative AMD

Moritz Lindner, Petra P. Fang, Julia S. Steinberg, Niklas Domdei, Maximilian Pfau, Tim U. Krohne, Steffen Schmitz-Valckenberg, Frank G. Holz, and Monika Fleckenstein

Department of Ophthalmology, University of Bonn, Bonn, Germany

Correspondence: Monika Fleckenstein, Department of Ophthalmology, University of Bonn, Ernst-Abbe-Str. 2, 53127 Bonn, Germany; Monika.Fleckenstein@ukb.uni-bonn.de.

Submitted: April 14, 2016
Accepted: October 17, 2016

Citation: Lindner M, Fang PP, Steinberg JS, et al. OCT angiography–based detection and quantification of the neovascular network in exudative AMD. *Invest Ophthalmol Vis Sci*. 2016;57:6342–6348. DOI:10.1167/iov.16-19741

PURPOSE. To investigate the potential of optical coherence tomography (OCT) angiography to detect and quantify the neovascular network in exudative AMD.

METHODS. Treatment-naïve eyes that were diagnosed with exudative AMD were prospectively examined by OCT angiography (OCT-A). The extent of the neovascular network was measured by three independent readers. Interclass-correlation coefficient and area overlap coefficients (OC) were calculated to assess locally precise agreement between measurements. As a reference for interreader agreement, the extent of the neovascular network was further measured on fluorescein angiography (FA) images.

RESULTS. A total of 31 eyes (27 patients, mean age 82.5 years, 15 female) were included in the study. Neovascularization subtype was classified as type I in 5, type II in 11, type III in 9, and mixed in 6 eyes, respectively. Interreader agreement for measurements of the neovascular network was 0.884 for OCT-A and 0.636 for FA. Overlap coefficient was 0.705 (interquartile [IQR]: 0.450–0.76) for OCT-A and 0.704 (IQR: 0.673–0.750) for FA, respectively. Area agreement was weaker in type III and mixed lesions.

CONCLUSIONS. Optical coherence tomography angiography–based measurements of the new vessel complex in neovascular AMD are feasible with interreader agreement comparable with the values obtained for FA. The results underscore the potential of OCT-A as a noninvasive diagnostic tool in neovascular AMD. Yet, further studies will be required to reveal the origin of poor agreement observed in single eyes and to advance OCT-A toward dependable use (e.g., in a reading center context).

Keywords: optical coherence tomography angiography, fluorescein angiography, age-related macular degeneration, choroidal neovascularization, full spectrum amplitude decorrelation

In industrialized countries, late stage AMD is the leading cause of legal blindness in the elderly.^{1,2} For neovascular AMD, the exudative late-stage manifestation associated with choroidal neovascularization (CNV), intravitreal injection of VEGF inhibitors (anti-VEGF) now represents an efficient therapeutic strategy.^{3,4} Neovascular AMD has been studied in detail using fluorescein angiography (FA) and indocyanine-green angiography (ICG-A).^{5,6} Recently, an anatomical classification for neovascular AMD has been proposed based on the additional information obtained from the cross-sectional lesion morphology as visualized by optical coherence tomography (OCT).^{7,8} However, conventional OCT devices do not allow direct visualization of the neovascular network; signs are rather indirect, such as intra- or subretinal fluid or pigment epithelial detachments. Fluorescein angiography is still considered the clinical gold standard when first diagnosing neovascular AMD.

Recently, amplitude decorrelation algorithms have enabled OCT devices to detect flow, thus allowing the visualization of the neovascular network.^{9–12} These new OCT angiography (OCT-A) devices are now available for clinical use. It has recently been shown that detailed visualization of the neovascular network in AMD is feasible^{10,13–15} and distinct morphologic subtypes of neovascularizations have been described.^{16–20} In addition, approaches have been made to

address morphologic differences between active, treatment requiring, and inactive CNV.^{21–23}

Quantification of the extent of neovascular networks is a task of major importance as lesion size has a well-recognized prognostic value.²⁴ In clinical routine^{24,25} as well as clinical trials²⁶ (ClinicalTrials.gov number, NCT02611778), this is currently being done employing FA. Despite an increasing number of reports on the appearance of neovascularization in OCT-A,^{17,27,28} there is no data available for the validation of OCT-A to determine the exact extent of the neovascular network. Yet, this is important for a future application of OCT-A in clinical routine and to convince cost payers in the health system to accept OCT-A as a diagnostic standard. The data would also be particularly important to validate this new method for future clinical trials using OCT-A-based parameters as outcome measures.

The present study aims to investigate the potential of OCT-A for reliable identification and quantification of the neovascular network in eyes with treatment-naïve exudative AMD. Values of intra- and interreader agreement are compared with the values obtained by measurements on FA. Furthermore, disease duration and neovascularization subtype are analyzed as possible factors influencing reproducibility of measurements.



METHODS

Ethics Statement

The study followed the tenets of the Declaration of Helsinki and was approved by the institutional review board (file no: 089/08). Informed written consent was obtained from each patient after explaining the nature and possible consequences of the study.

Patient Selection and Image Acquisition

Patients were consecutively recruited from the outpatient clinic of the Department of Ophthalmology, University of Bonn (Bonn, Germany), a tertiary care referral center for macular disorders. Patients diagnosed with treatment-naïve neovascular AMD based on funduscopy, spectral domain OCT and FA imaging were included in this study. Exclusion criteria encompassed the presence of other retinal diseases that could possibly confound the observation such as diabetic maculopathy or retinal vein occlusion.

Clinical routine examination included best corrected visual acuity (BCVA), slit-lamp examination, dilated indirect ophthalmoscopy, a $20^\circ \times 15^\circ$ spectral domain OCT volume scan (consistent of ≥ 19 single B scans) and FA using an OCT device (Spectralis HRA+OCT; Heidelberg Engineering, Heidelberg, Germany) confocal scanning laser ophthalmoscopy system and fluorescein 5 mL (Alcon Pharma GmbH, Freiburg, Germany). After confirmation of the diagnosis “exudative AMD,” patients were asked to participate in the study and informed consent was obtained. Optical coherence tomography angiography, which was not part of the standard clinical care, was then performed as the unique study procedure. When both eyes of a patient met the inclusion criteria, both eyes were included in the analysis.

Acquisition of OCT Angiography

After informed consent was obtained, OCT-A images were acquired using a Spectralis HRA+OCT (Heidelberg Engineering) combined OCT and confocal laser-scanning ophthalmoscopy (cSLO) system. The device uses an 870-nm light source and an optical system that allows for acquisition of $85k \times s^{-1}$ A-scans. Image stabilization and averaging is achieved by active eye tracking and a real-time alignment algorithm. Acquisition of an OCT angiogram is based on a full-spectrum amplitude decorrelation algorithm calculating a differential image of sequential B-scans obtained from the same position. The principles of the full-spectrum amplitude decorrelation algorithm (FSADA) and angiogram acquisition as performed using the OCT device (Heidelberg Engineering) are described in detail elsewhere.²⁹ Briefly, the difference between two images represents movement, in the retina essentially representing blood flow. In contrast to the currently more widely known split-spectrum amplitude decorrelation algorithm (SSADA) in FSADA, each B-scan is not spectrally segregated into multiple images but rather amplitude decorrelation is obtained between sequential “full spectrum” B-scans. Signal-to-noise ratio is improved by averaging multiple B-scans from a similar anatomic position. The scan volume was adjusted by discretion of the examiner to cover a volume of 5×15 to 15×15 . The distance between two single B-scans in the volume was set to 11 μm . By software processing this volume scan renders an *en face* image based on the minimum, maximum, or mean intensity of the pixels within a manually defined slab.

Image Grading

Grading of the neovascular network based on OCT-A and FA was performed by three independent readers (ML, JS, PF) who

were blinded to the results of each other and any other imaging modality.

We viewed OCT-A and FA using imaging software (Heidelberg Eye Explorer, version 1.9.201.0; viewing module version 6.0.205.2 [OCT-A] and 6.3.2.0 [FA]; Heidelberg Engineering) and readers were asked to delineate and measure the area of the neovascular network using the “draw region” tool. For OCT-A images, the neovascular network was visualized and quantified in the *en face* projection at its greatest horizontal dimension at the discretion of the reader. Standards for rendering and visualization for OCT-A slabs were not yet implemented into the version of the imaging software (Heidelberg Engineering) used in the current analysis. Therefore, manual adjustment of the settings for OCT-A contrast, method of projection (minimum, maximum or mean intensity) as well as thickness and location of the slab was performed at the discretion of the reader. In case the readers considered that no neovascular network was visible, they could omit this particular grading. To obtain values for intrareader agreement, one reader (ML) graded both, OCT-A and FA and, twice. Exemplary measurements are given in Figure 1.

For fluorescein angiography images, delineation and measurements of the neovascular network were performed analogue to the procedures defined in the Comparison of Age-related Macular Degeneration Treatments Trials study.²⁶ In brief, for type II lesions, an image acquired right before the onset of leakage was chosen. For type I lesions, an image was chosen showing fully developed staining. In the current study, area measurements of type III neovascularizations were performed according to the procedure chosen for type II lesions by Grunwald et al.²⁶ These procedures allow for reducing inclusion of concomitant leakage into measurements of the new vessel complex size.

Images of OCT-A and FA, with the outlined area of the neovascular network, were saved as digital image files (TIFF) for further processing and all values, including the size of the neovascular network and the parameters used for visualization, were recorded in a spreadsheet application.

The neovascularization subtypes were classified in accordance with the previously described scheme by Freund et al.^{7,8} by two of the readers (ML, MP) and a senior reader (MF) in case of discrepancy. In brief, type I neovascularizations were defined by an elevated RPE line in the OCT, often with subretinal fluid and an early stippled hyperfluorescence with mild to moderate staining or leakage in the late phase observed in the FA. Type II was defined as showing hyperreflective material above the RPE and intra- or subretinal edema together with early lacy pattern hyperfluorescence and intense leakage in the FA. Type III was defined by intraretinal hyperreflective spots and cysts on OCT together with early focal leakage on the FA.⁸

Image Processing and Statistical Analysis

Data were analyzed using R statistical software.³⁰ Intra- and interobserver agreement for size of the neovascular network was assessed using the interclass correlation coefficient (ICC).³¹ To analyze any systematic disagreement between two measurements of the same reader or between the readers, the descriptive method of Bland and Altman was additionally employed.³² In brief, in Bland-Altman-plots the difference in measurements gained by two readers is plotted against the mean of the measurements. A value of 0 on the y-axis indicates perfect agreement. Dashed lines indicate mean difference and the limits of agreement.

Though ICC and Bland-Altman statistics are common tools used to address the agreement between examiners with regard to retinal imaging, measuring the same size does not

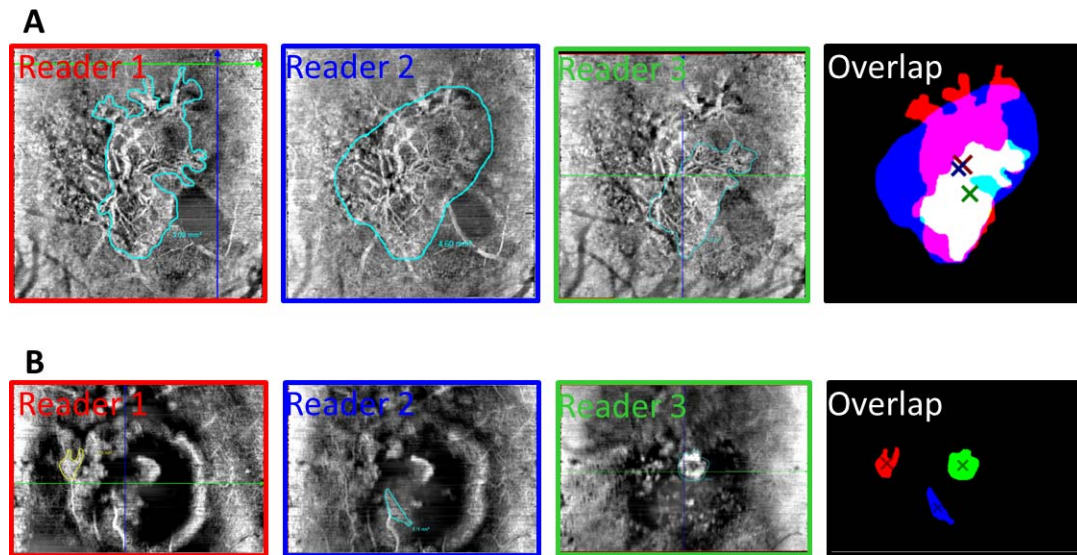


FIGURE 1. Two examples of neovascular lesions as measured by the three independent readers. For illustration, each reader was assigned a color (red, blue, green). In the overlap image combination colors suggest overlap between the readers. (A) Eye with an intermediate interreader agreement is shown ($OC = 0.657$), exemplifying the influence of optimal slab elicitation and exact CNV delineation. (B) Shows an eye with $OC = 0$, suggesting that readers did identify different presumptive abnormalities as neovascularization. Image artefacts³⁷ not flow signal through neovascularization drove the readers to demark a certain region in the image. Crosses mark the centroid position of corresponding areas.

essentially mean the same structure was really assessed. We therefore additionally assessed pixelwise area correlation applying a colocalization coefficient.³³ For each eye, FA and OCT-A images with the outlined neovascular network were registered on each other and cropped to the area of the *en face* OCT-A image using ImageJ, version 1.49g (<http://imagej.nih.gov/ij/>; provided in the public domain by the National Institutes of Health, Bethesda, MD, USA).^{34,35} Resulting images were converted into binary images, where the area marked as neovascular network appeared black using a color-threshold approach (Figure 2). These images were then transferred to a computing environment (MATLAB, version R2014a; MathWorks, Inc., Natick, MA, USA) to calculate overlap coefficients (OC).³³ An OC of 1 implies a perfect agreement; a value of 0 implies no overlap of the measured areas at all.

Values given in the manuscript represent medians and corresponding upper and lower quartiles if not indicated otherwise. If applicable, variances between groups were assessed using a 2-way ANOVA or Kruskal-Wallis-Test as appropriate. When represented in Boxplots, black bars indicate the median; hinges represent the first and third quartile. Whiskers range from the highest to the lowest value within the 1.5-fold IQR of the hinge. Dots represent the individual values.

RESULTS

A total of 31 eyes (27 patients, 15 female) were included in the study. Mean age of patients was 82.5 years (range: 67.4–91.7 years) and median BCVA at the day of examination was 0.40 (IQR: 0.18–0.50) logMAR. In 18 eyes, patients reported no symptoms or a symptom onset of <3 months; for seven eyes, patients reported a symptom onset of >3 months. In 6 eyes, patients did not remember the date of symptom onset. According to the anatomical classification (based on FA and conventional OCT),⁸ the neovascularization subtype was graded as follows: type I in 5 eyes (16%); type II in 11 eyes (35%); type III in 9 eyes (29%); and mixed in 6 eyes (19%).

In 12 eyes, the neovascular network exceeded the image-frame on the OCT-A image. These eyes were not included in the further analyses.

Analysis of the remaining 19 eyes (three type I, seven type II, six type III, and three mixed; disease duration: <3 months in 11 eyes, >3 months in 5 eyes, unknown in 3 eyes) revealed the following results: The median lesion size measured on OCT-A was 0.550 mm² (IQR: 0.303–0.685 mm²). For fluorescein angiography, the median neovascular network size was 0.447 mm² (IQR: 0.212–0.602 mm²). The intraclass correlation coefficient for intrareader agreement was 0.884 for OCT-A and 0.636 for FA. The descriptive method by Bland and Altman did not reveal any systematic differences in measurement of lesion size in either method (Figs. 3A, 3B). For interreader agreement the ICC between the three readers was 0.670 for OCT-A and 0.748 for FA, respectively (Fig. 4A). Bland-Altman plots suggested that there was an overall tendency toward a larger disagreement between the readers with increasing lesion size, predominantly in OCT-A but also in FA (Figs. 3C–H).

Comparison of the OC for area agreement between the three readers revealed the following results: The median interreader OC was 0.705 (IQR: 0.450–0.793) for OCT-A and 0.704 (IQR: 0.673–0.750) for FA ($P = 0.543$; Figs. 2, 4B).

On optical coherence tomography angiography, median lesion size for type I, type II, type III, and mixed lesions were 0.700 (IQR: 0.520–1.901); 0.580 (IQR: 0.477–0.905); 0.288 (IQR: 0.088–0.499); and 0.630 (IQR: 0.393–0.650), respectively. Values of OC differed between lesion subtypes with median OC values of 0.760 (IQR: 0.709–0.765) for type I; 0.801 (IQR: 0.763–0.861) for type II; 0.559 (IQR: 0.477–0.641) for type III; and 0.278 (IQR: 0.139–0.360) for mixed lesions. However, these differences were not significant (Kruskal-Wallis test).

Nor was there significant dependency of OC on symptom duration. For patients who experienced no symptoms or symptoms for less than 3 months, the median OC was 0.657 (IQR: 0.458–0.765), while it was 0.600 (IQR: 0.281–0.838) in those with a symptom onset > 3 months ago.

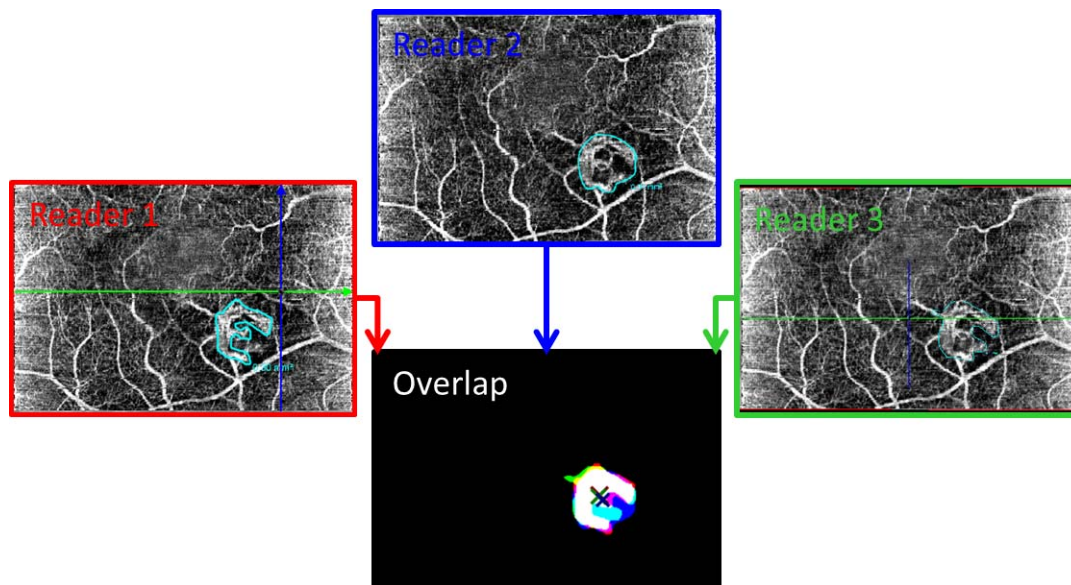


FIGURE 2. Illustration of image processing applied to calculate the area OC. Neovascular lesions were outlined by each reader (readers 1–3), converted into binary images and OCs between each of the readers were calculated. For illustration, each reader was assigned a color. In the overlap image, an overlap of the areas as demarked by each of the three readers appears as *white*, an overlap between two readers as *yellow*, *magenta*, and *cyan*. Areas of no overlap appear as *red*, *blue*, and *green*, corresponding to the color assigned to each reader. *Crosses* mark the centroid position of corresponding areas.

DISCUSSION

The current study demonstrates that OCTA-based measurements of neovascular lesions in exudative AMD are feasible with an intra- and interreader agreement, comparable with the values obtained for FA within this study. Although the overall high ICC and OC for interreader area agreement indicates the validity of OCTA for the detection of the neovascular network, low agreement in single eyes, particularly with type III and mixed lesions, points to distinct challenges implicated with this novel imaging modality.

For type III lesions, a recent study even reported that only 34% of the lesions could be visualized on OCTA.³⁶ This may be explained by the lack of detecting leakage by OCTA that may obscure the presence of small neovascular lesions that would have been detected by FA mainly by tracing back leakage.

Furthermore, displaying the third-dimension by OCTA also represents a potential additional source of disagreement between readers concerning lesion delineation, and would especially influence measurements in lesions that span the retina in axial directions (predominantly type III and mixed lesions). Strategies for volumetric analyses are not established, yet. Therefore, a slab has to be defined where the two-dimensional measurements are performed. In the setting of this study, readers were allowed to manually adjust the parameters for generation of the en face OCTA slabs (namely: contrast, method of projection [minimum, maximum or mean intensity] as well as thickness and axial location of the slab). This became necessary as no standard settings for evaluation on neovascular membranes were implemented yet in the prototypic OCTA viewing software used in this study. An advantage of this strategy was that correction of projection artefacts and minor segmentation inaccuracies were feasible. Indeed, this may represent a source of disagreement between readers in the current study. Improvement of algorithms for automated slab generation may certainly decrease inter-reader variability.

The weaker OC in type III lesion delineation in the current analysis may also be due to the on average smaller lesion size compared with other subtypes. This may in part be explained

by the fact that a single pixel of disagreement as depicted in the en face image has a stronger relative impact on OC. Misinterpretation due to decreased quality or of imaging artifacts (e.g., signal noise falsely detected as movement by the decorrelation algorithm), would therefore have a larger implication.

The capacity of OCTA to visualize flow is limited to a certain range of flow velocities (minimum: 0.5–2 mm/s, saturation: 9 mm/s estimated for current devices) also needs to be considered.⁹ In theory, it is possible that certain neovascular networks (or at least parts of them) have flow velocities below the detection limit. Such lesions would be invisible on OCTA. The exact range of detectable flow rates is determined by the physical specifications of an individual device and the employed algorithm for angiogram generation. Various OCTA devices using differing methods for the generation of angiography images are currently available. In a clinical context, FSADA or SSADA⁹ that interpret changes observed between two images sequentially obtained from the same location as movement are of major importance.^{11,37} The Spectralis HRA+OCT2 uses a “full-spectrum” decorrelation algorithm, while the SSADA is implemented e.g. in the RTVue XR Avanti (Optovue, Inc., Fremont, CA, USA). A novel algorithm using signal amplitude and phase information (“OMAGC”) has been recently implemented in the ZEISS AngioPlex (Carl Zeiss Meditec, Jena, Germany).³⁸ Ratio-based analysis of sequential OCT B-scans for generation of OCTA data is employed by the Topcon (Topcon Corporation, Tokyo, Japan) devices.³⁹ The impact of different OCTA generation methods has recently been investigated in single individuals.⁴⁰ Future studies on larger cohorts will elucidate the advantages of the different algorithms and devices used in clinical routine.

Besides the acquisition algorithm, other factors like axial and lateral resolution, maximal scanning volume size, image averaging and segmentation procedures will influence diagnostic accuracy and interreader agreement for each particular device. With regard to segmentation, the OCT software (Heidelberg Engineering) to date provides both predefined slabs for data assessment, but also easily accessible manual

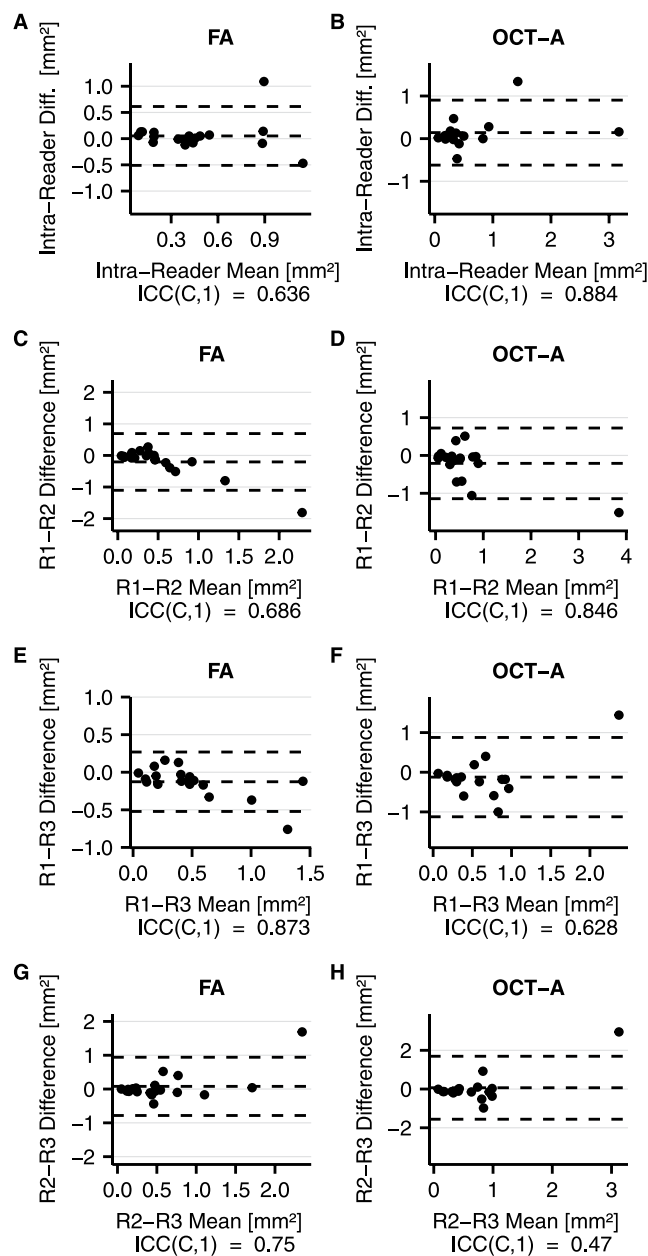


FIGURE 3. Bland-Altman plots for FA (A, C, E, G) and OCT-A (B, D, F, H). Bland-Altman plots depict the difference between two measurements as a function of their mean. (A, B) Bland-Altman plots are drawn for the first and the second grading of the same reader. (C-H) Difference between each pair of readers is shown. Corresponding ICC are given below each graph. R1, reader 1; R2, reader 2; R3, reader 3.

adjustment tools; on the other hand the SD-OCT device (Optovue, Inc.) and OCT-A software (Carl Zeiss Meditec) software puts higher emphasis on predefined slabs. The use of predefined slabs will generally increase the agreement between different users; however, the chance to easily access tools for manual adjustment of these slabs (as frequently used by the readers in this study) might increase the overall diagnostic accuracy in clinical routine. Accuracy of segmentation algorithms and in particular their reliability in the presence of any pathologic finding is key for the detection of neovascularization. Faulty segmentation may either visualize vessels away from their actual anatomic position and thereby simulate the presence of a neovascularization or, conversely,

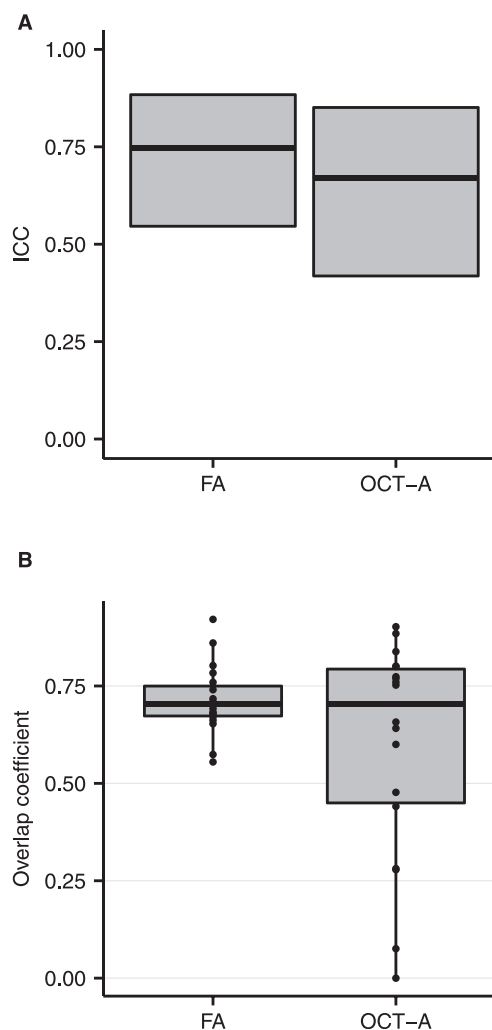


FIGURE 4. Box plots illustrating (A) ICC and (B) the area OC between the three readers for FA and OCT-A, respectively. Note that in (A) horizontal bars represent the mean and hinges the upper and lower bounds of the confidence interval.

lead to nonvisualization of actually existing pathologic vessels.^{11,37} To the best of our knowledge, none of the currently used segmentation algorithms is validated in terms of reliability in presence of pathologic findings. This will be an important task for future studies.

With regard to scanning volume size, this study underscores that volumes of 5×15 to 15×15 (= approximately 1×3 to 3×3 mm in an emmetropic eye) may be insufficient for the assessment of the entire neovascular network. Notably, in the current analysis, in 12 of 31 eyes the neovascularization exceeded the image frame on OCT-A. Therefore, it appears reasonable to apply larger scanning volume sizes to assess the neovascular membrane in future trials as well as in clinical routine.

Of practical interest is also the time required for acquisition of an OCT-A. As generation of OCT-A does not depend on the flooding kinetics of any dye, acquisition times are generally shorter than for FA or ICG-A. The exact acquisition time obviously depends on the acquisition parameters (scan volume, scan resolution, numbers of scans averaged) elicited and also the device employed (scan speed, speed of eye tracking system).

There are several limitations to the design of the current study. It must be considered that all eyes included in this study have received the diagnosis of exudative AMD in clinical routine based on FA. This might have led to an a priori exclusion of eyes where the neovascularization was poorly visualized on FA. In future studies it needs to be further assessed if, and under what conditions, neovascularizations are not, or only poorly, visualized by OCT-A to avoid erroneous diagnosis in clinical routine as well as in clinical trials.

The fact that the readers knew that each included eye had presented with signs of neovascularization on FA obviously represents a bias. This might have influenced the readers to outline and measure presumptive structures in eyes which they might otherwise not have classified as a neovascular lesion. However, the overall high OC values for area colocalization show that readers—even in doubtful situations—generally chose identical lesions to represent neovascular complexes.

Published data on the agreement of area quantification between different readers in FA is sparse. In scanning laser ophthalmoscopy images, Vujosevic and coworkers⁴¹ obtain a κ value of 0.45 comparing the categorized values for neovascular lesion diameter obtained by two readers. Comparable values were obtained for fluorescein photographs categorizing by disk areas ($\kappa = 0.4$).⁴² These categorical values are not directly comparable with the continuous values for agreement obtained here, but κ values of 0.4 to 0.45 would rather correspond to ICC values slightly below those obtained in the current analysis. In this context it has to be considered that on FA, quantification of the extent of the actual neovascular network is challenging due to leakage. Therefore, FA images of specific time-points were chosen for quantification of the distinct lesion subtypes as previously described by Grunwald and coworkers.²⁶ By applying this strategy, ICC values for inter- and intrareader agreement of >0.9 were obtained,²⁶ that were slightly higher than in the current analysis.

Due to potential inclusion of areas of pure leakage, direct comparison of absolute values of the size of the neovascular network measured on FA and OCT-A, does not appear to be reasonable. Notably, in the current analysis, median lesion size values were smaller on FA than on OCT-A, suggesting further factors influencing differential results. Indocyanine-green angiography would be superior as an imaging modality to compare absolute sizes of the neovascular network with OCT-A. However, ICG-A has not been part of this study. Instead, the present study was particularly designed to assess the feasibility of lesion quantification in OCT-A (as measured by ICC and OC) and to compare with values for ICC and OC obtained with FA, which is the current standard in clinical routine care^{24,25} as well as clinical trials²⁶ (ClinicalTrials.gov number, NCT02611778).

In summary, this study demonstrates that detection and quantification of neovascular lesions in exudative AMD using OCT-A achieve a good agreement between different examiners. Degrees of agreement were overall comparable to FA-based measurements. Yet, there were several eyes with poor agreement of delineation of the neovascular network based on OCT-A. The underlying reasons need to be focused in future analyses. Overall, the present results underscore the potential of OCT-A as non-invasive diagnostic tool in exudative AMD.

Acknowledgments

Supported by the BONFOR GEROK Program of the Faculty of Medicine, University of Bonn, Grant No. O-137.0020 (ML) and the German Research Foundation (DFG), Grant No. FL658/4-1 (MF) and HA5323/5-1. The authors alone are responsible for the content and writing of the paper.

Disclosure: **M. Lindner**, Heidelberg Engineering (F), Carl Zeiss Meditec (F, D), Optos (F), Genentech/Roche (F), Alimera Sciences (R); **P.P. Fang**, Heidelberg Engineering (F); **J.S. Steinberg**, Heidelberg Engineering (F), Carl Zeiss Meditec (F), Optos (F); **N. Domdei**, Heidelberg Engineering (F, R), Carl Zeiss Meditec (F, R), Optos (F), Alimera Sciences (R); **M. Pfau**, Bayer (R), Carl Zeiss Meditec (F), Heidelberg Engineering (F), Optos (F); **T.U. Krohne**, Heidelberg Engineering (F, R), Alcon (F), Novartis (F, R), Bayer (R); **S. Schmitz-Valckenberg**, Heidelberg Engineering (F, R), Carl Zeiss Meditec (F), Optos (F), Genentech/Roche (F), Bayer (F, R), Allergan (F), Formycon (F), Novartis (F); **F.G. Holz**, Heidelberg Engineering (C, F), Carl Zeiss Meditec (F), Optos (F), Genentech/Roche (C), Alcon (C), Allergan (C), Bayer (C); **M. Fleckenstein**, Heidelberg Engineering (F, R), Carl Zeiss Meditec (F), Optos (F), Genentech/Roche (F, R), Mertz (C), Novartis (R), Bayer (R), P

References

- Congdon N, O'Colmain B, Klaver CC, et al. Causes and prevalence of visual impairment among adults in the United States. *Arch Ophthalmol*. 2004;122:477-485.
- Resnikoff S, Pascolini D, Etya'ale D, et al. Global data on visual impairment in the year 2002. *Bull World Health Org*. 2004;82:844-851.
- Martin DF, Maguire MG, Fine SL, et al. Ranibizumab and bevacizumab for treatment of neovascular age-related macular degeneration: two-year results. *Ophthalmology*. 2012;119:1388-1398.
- Rofagha S, Bhisitkul RB, Boyer DS, Sadda SR, Zhang K. Seven-year outcomes in ranibizumab-treated patients in ANCHOR, MARINA, and HORIZON: a multicenter cohort study (SEVEN-UP). *Ophthalmology*. 2013;120:2292-2299.
- Macular Photocoagulation Study Group. Subfoveal neovascular lesions in age-related macular degeneration. Guidelines for evaluation and treatment in the macular photocoagulation study. *Arch Ophthalmol*. 1991;109:1242-1257.
- Yannuzzi LA, Negrao S, Iida T, et al. Retinal angiomatous proliferation in age-related macular degeneration. *Retina*. 2001;21:416-434.
- Freund KB, Zweifel SA, Engelbert M. Do we need a new classification for choroidal neovascularization in age-related macular degeneration? *Retina*. 2010;30:1333-1349.
- Jung JJ, Chen CY, Mrejen S, et al. The incidence of neovascular subtypes in newly diagnosed neovascular age-related macular degeneration. *Am J Ophthalmol*. 2014;158:769-779.e762.
- Jia Y, Tan O, Tokayer J, et al. Split-spectrum amplitude-decorrelation angiography with optical coherence tomography. *Opt Exp*. 2012;20:4710-4725.
- Fang PP, Lindner M, Steinberg JS, et al. Clinical applications of OCT angiography [in German]. *Ophthalmologie*. 2016;113:14-22.
- Fang PP, Harmening WM, Muller PL, Lindner M, Krohne TU, Holz FG. Technical principles of OCT angiography [in German]. *Ophthalmologie*. 2016;113:6-13.
- de Carlo T, Romano A, Waheed N, Duker J. A review of optical coherence tomography angiography (OCTA). *Int J Retina Vitreous*. 2015;1:5.
- Jia Y, Bailey ST, Wilson DJ, et al. Quantitative optical coherence tomography angiography of choroidal neovascularization in age-related macular degeneration. *Ophthalmology*. 2014;121:1435-1444.
- Moult E, Choi W, Waheed NK, et al. Ultrahigh-speed swept-source OCT angiography in exudative AMD. *Ophthalmic Surg Lasers Imaging Retina*. 2014;45:496-505.
- Marques JP, Costa JE, Marques M, Cachulo ML, Figueira J, Silva R. Sequential morphological changes in the CNV net after

- intravitreal anti-VEGF evaluated with OCT angiography. *Ophthalmic Res.* 2016;55:145–151.
16. Kuehlewein L, Sadda SR, Sarraf D. OCT angiography and sequential quantitative analysis of type 2 neovascularization after ranibizumab therapy. *Eye (Lond)*. 2015;29:932–935.
 17. Kuehlewein L, Bansal M, Lenis TL, et al. Optical coherence tomography angiography of type 1 neovascularization in age-related macular degeneration. *Am J Ophthalmol.* 2015;160:739–748.e732.
 18. Liang MC, Witkin AJ. Optical coherence tomography angiography of mixed neovascularizations in age-related macular degeneration. *Dev Ophthalmol.* 2016;56:62–70.
 19. Iafe NA, Phasukkijwatana N, Sarraf D. Optical coherence tomography angiography of type 1 neovascularization in age-related macular degeneration. *Dev Ophthalmol.* 2016;56:45–51.
 20. Souied EH, El Ameen A, Semoun O, Miere A, Querques G, Cohen SY. Optical coherence tomography angiography of type 2 neovascularization in age-related macular degeneration. *Dev Ophthalmol.* 2016;56:52–56.
 21. Coscas GJ, Lupidi M, Coscas F, Cagini C, Souied EH. Optical coherence tomography angiography versus traditional multimodal imaging in assessing the activity of exudative age-related macular degeneration: a new diagnostic challenge. *Retina.* 2015;35:2219–2228.
 22. Palejwala NV, Jia Y, Gao SS, et al. Detection of nonexudative choroidal neovascularization in age-related macular degeneration with optical coherence tomography angiography. *Retina.* 2015;35:2204–2211.
 23. Lumbroso B, Rispoli M, Savastano MC, Jia Y, Tan O, Huang D. Optical coherence tomography angiography study of choroidal neovascularization early response after treatment. *Dev Ophthalmology.* 2016;56:77–85.
 24. Schmidt-Erfurth U, Chong V, Loewenstein A, et al. Guidelines for the management of neovascular age-related macular degeneration by the European Society of Retina Specialists (EURETINA). *Br J Ophthalmol.* 2014;98:1144–1167.
 25. AAO Retina/Vitreous PPP Panel. Age-related macular degeneration PPP. Available at: <http://www.aao.org/preferred-practice-pattern/age-related-macular-degeneration-ppp-2015>. Accessed: August 26, 2016.
 26. Grunwald JE, Daniel E, Ying GS, et al. Photographic assessment of baseline fundus morphologic features in the Comparison of Age-Related Macular Degeneration Treatments Trials. *Ophthalmology.* 2012;119:1634–1641.
 27. Muakkassa NW, Chin AT, de Carlo T, et al. Characterizing the effect of anti-vascular endothelial growth factor therapy on treatment-naïve choroidal neovascularization using optical coherence tomography angiography. *Retina.* 2015;35:2252–2259.
 28. de Carlo TE, Bonini Filho MA, Chin AT, et al. Spectral-domain optical coherence tomography angiography of choroidal neovascularization. *Ophthalmology.* 2015;122:1228–1238.
 29. Coscas G, Lupidi M, Coscas F. Heidelberg Spectralis optical coherence tomography angiography: technical aspects. *Dev Ophthalmol.* 2016;56:1–5.
 30. R Development Core Team. R: A language and environment for statistical computing. Vienna, Austria: R Foundation for Statistical Computing; 2010.
 31. Bartko JJ. The intraclass correlation coefficient as a measure of reliability. *Psychol Rep.* 1966;19:3–11.
 32. Bland JM, Altman DG. Statistical methods for assessing agreement between two methods of clinical measurement. *Lancet.* 1986;1:307–310.
 33. Manders EMM, Verbeek FJ, Aten JA. Measurement of colocalization of objects in dual-colour confocal images. *J Microsc.* 1993;169:375–382.
 34. Bolte S, Cordelières FP. A guided tour into subcellular colocalization analysis in light microscopy. *J Microsc.* 2006;224:213–232.
 35. Schindelin J, Arganda-Carreras I, Frise E, et al. Fiji: an open-source platform for biological-image analysis. *Nat Methods.* 2012;9:676–682.
 36. Kuehlewein L, Dansingani KK, de Carlo TE, et al. Optical coherence tomography angiography of type 3 neovascularization secondary to age-related macular degeneration. *Retina.* 2015;35:2229–2235.
 37. Spaide RF, Fujimoto JG, Waheed NK. Image artifacts in optical coherence tomography angiography. *Retina.* 2015;35:2163–2180.
 38. Rosenfeld PJ, Durbin MK, Roisman L, et al. ZEISS Angioplex spectral domain optical coherence tomography angiography: technical aspects. *Dev Ophthalmol.* 2016;56:18–29.
 39. Stanga PE, Tsamis E, Papayannis A, Stringa F, Cole T, Jalil A. Swept-source optical coherence tomography angiography (Topcon Corp, Japan): technology review. *Dev Ophthalmol.* 2016;56:13–17.
 40. Gorczynska I, Migacz JV, Zawadzki RJ, Capps AG, Werner JS. Comparison of amplitude-decorrelation speckle-variance and phase-variance OCT angiography methods for imaging the human retina and choroid. *Biomed Opt Exp.* 2016;7:911–942.
 41. Vujosevic S, Vlacik V, Bird AC, Leung I, Dandekar S, Peto T. Combined grading for choroidal neovascularisation: colour fluorescein angiography and autofluorescence images. *Graefes Arch Clin Exp Ophthalmol.* 2007;45:1453–1460.
 42. Friedman SM, Margo CE. Choroidal neovascular membranes: reproducibility of angiographic interpretation. *Am J Ophthalmol.* 2000;130:839–841.